

Original paper

Chemical and spectroscopic characterization of tourmalines from the Mata Azul pegmatitic field, Central Brazil

Simone F. da SILVA^{1,2*}, Márcia A. MOURA², Hudson de A. QUEIROZ², José D. ARDISSON³

¹ Instituto Federal de Minas Gerais, Campus Congonhas, Avenida Michel Pereira de Souza, 3007, Campinho, 36415-000 Congonhas, Minas Gerais, Brazil; simone.geologia@gmail.com

² Instituto de Geociências, Universidade de Brasília, Campus Darcy Ribeiro, Asa Norte, 70910-900 Brasília, Distrito Federal, Brazil

³ Centro de Desenvolvimento de Tecnologia Nuclear (CDTN), Laboratório de Física Aplicada, Rua Prof. Mário Werneck, 30161970, Belo Horizonte, Minas Gerais, Brazil

* Corresponding author



This study characterizes natural black, blue, dark green, light green and pink tourmalines from granitic pegmatites of the Mata Azul Pegmatitic Field in central Brazil. The differences were assessed by applying electron-microprobe analysis as well as Mössbauer and optical spectroscopies. Mineral chemistry data show an increasing Mn/(Mn + Fe) atomic ratio as follows: black (0.01–0.02), blue (0.04–0.05), dark green (0.09–0.21), light green (0.33–0.42) and pink (0.68–1.00). The Mössbauer spectroscopy results show the presence of Fe²⁺ (doublets with isomer shift (δ): 1.04–1.15 mm/s) for the black, blue, light green and dark green tourmalines. Fe²⁺ is found in three different environments that are identified by quadrupole splitting (Δ) of 2.38–2.49 mm/s for the first, $\Delta = 2.13$ –2.34 mm/s for the second, and $\Delta = 1.54$ –1.71 mm/s for the third. The black sample spectrum has an additional fourth doublet ($\delta = 0.78$ mm/s, $\Delta = 1.22$ mm/s) that is assigned to an electron delocalization between Fe²⁺ and Fe³⁺.

In the studied samples, the black color results most likely from high absorbance in all the visible spectra caused by Fe²⁺–Fe³⁺ intervalence charge transfer (IVCT) (780 nm), Fe²⁺ d–d transitions (730 nm, 670 nm), Fe²⁺–Ti⁴⁺ IVCT (430 nm) and transitions related to Mn cations (550 nm). Blue is differentiated from green colors by a higher absorbance in the 730 nm region (Fe²⁺ d–d transitions), and a higher FeO content, as well as a lower absorbance in the 430 nm region and a lower TiO₂ content. The green colors are associated with the absorption bands at 730 nm (Fe²⁺ d–d transitions) and 430 nm (Fe²⁺–Ti⁴⁺ IVCT). The light green color exhibited a lower intensity of these bands compared to that of the dark green color, and an additional band at 320 nm (Mn²⁺–Ti⁴⁺ IVCT). The pink color results from the high degree of Mn–Fe fractionation but it was not possible to assure the oxidation states of the Mn cations.

Keywords: mineral color, tourmaline, electron microprobe, Mössbauer spectroscopy, optical spectroscopy

Received: 28 September, 2017; accepted: 1 June, 2018; handling editor: J. Cempírek

The online version of this article (doi: 10.3190/jgeosci.258) contains supplementary electronic material.

1. Introduction

Tourmaline-supergrupp minerals are borosilicates with a complex structure where a large variety of chemical elements can be incorporated by simple or coupled substitutions. For this reason, tourmalines feature a wide range of colors and are frequently used as a gemstone. The general formula of tourmaline-supergrupp minerals is $XY_3Z_6T_6O_{18}(BO_3)_3V_3W$, where the most common ions or vacancies (\square) at the individual sites are: $X = Na^+$, Ca^{2+} , K^+ or \square , $Y = Fe^{2+}$, Mg^{2+} , Mn^{2+} , Al^{3+} , Li^{1+} , Fe^{3+} , Cr^{3+} , Ti^{4+} and V^{3+} , $Z = Al^{3+}$, Fe^{3+} , Mg^{2+} , Cr^{3+} , and V^{3+} , $T = Si$, Al and B , $B = B$, $V = OH^-$ and O^{2-} , $W = OH^-$, F^- and O^{2-} (Henry et al. 2011; Henry and Dutrow 2012).

The color of tourmaline-supergrupp minerals is influenced mainly by amount of transition metal cations and their distribution between the Y and Z sites, in some cases also by the presence of electron or hole traps (Krambrock

et al. 2004). Therefore, full chemical and spectroscopic characterization of tourmalines is essential in order to determine the cause of their color; this has been topic of many studies (e.g., Castañeda 2002; Krambrock et al. 2002, 2004; Liu et al. 2011; Taran et al. 2015; Manee-wong et al. 2016).

In this paper, we present a study on causes of color in tourmalines from the Mata Azul Pegmatitic Field, Tocantins and Goias, central Brazil (Queiroz 2016, Queiroz and Botelho in print). We performed chemical and spectroscopic characterization of the tourmalines using electron-microprobe analysis (EMPA) optical spectroscopy in ultraviolet–visible range (UV-VIS) and Mössbauer spectroscopy, which are all well-established techniques in tourmaline color characterization. This is the first advanced multi-analytical study on tourmalines from the Mata Azul region, an important artisanal mining district in Brazil in the 1980s.

2. Geological setting

The Mata Azul Pegmatitic Field (central Brazil) (Queiroz 2016, Queiroz and Botelho in print) is located in the extensive Northern Brasília Fold Belt (Dardenne 2000; de Almeida et al. 1981), which is part of the Neoproterozoic Tocantins Province. This is a major orogenic system built by the Araguaia, Paraguaia and Brasília belts formed due to the collision of the Amazon Craton, the São Francisco Craton and the Paranapanema Block (Valeriano et al. 2004).

The Mata Azul Pegmatitic Field was defined by Queiroz (2016), who distinguished and characterized in detail barren pegmatites, beryl-bearing pegmatites and tourmaline-bearing pegmatites, typically with exposures ranging from tens to hundreds of square meters. Based on the Černý and Ercit (2005) classification, both the beryl- and the tourmaline-bearing pegmatites belong to the rare-element (REL) class and the REL–Li subclass of granitic pegmatites; most of the pegmatites once explored for tourmaline in this region belong to the complex type and classify as elbaite-subtype pegmatites, and most of those explored for beryl belong to the beryl type, beryl–columbite–phosphate subtype. Their source is considered to be the Mata Azul granitic Suite. They are intrusive in the metasedimentary rocks of the Serra da Mesa Group and the Ticunzal Fm. as well as in the peraluminous granites of the Aurumina Suite (Queiroz 2016; Queiroz and Botelho 2017, in print; Fig. 1). The Ticunzal Fm. and the Aurumina Suite are part of the basement of the Northern Brasília Belt external zone.

The *Ticunzal Fm.* is dominated by paragneisses and mica-graphite schists, with mineral assemblages indicating retrograde metamorphism under greenschist-facies conditions, and also presents tourmaline schists, minor quartzites and rare metaconglomerates. The Aurumina Suite is composed of peraluminous granites, tonalities/granodiorites with mineral assemblage of magmatic muscovite ± biotite ± garnet and discrete xenocrystic graphite lamellae. These granitic rocks are intrusive in the Ticunzal Fm. and have U–Pb ages on zircon between 2.11 and 2.16 Ga (Alvarenga et al. 2007; Cuadros et al. 2017a, b).

The *Serra da Mesa Group* has been interpreted as a metamorphosed marine sequence where sediments were deposited in a silicic–carbonate platform (Marques 2009) between 1.57 and 1.47 Ga (Dardenne 2000).

The Mata Azul Suite is composed of granites containing quartz, perthitic microcline, oligoclase, muscovite, biotite, tourmaline, beryl, garnet and tantalite and post-tectonic pegmatites (Lacerda Filho et al. 1999; Polo and Diener 2013). Some leucogranites in this unit were classified by Queiroz (2016) as peraluminous with geochemical signatures typical of LCT granites and pegmatites, following Černý (1990, 1991). Recently, Queiroz and

Botelho (in print) reported U–Pb ages on monazite of 519.9 ± 2.8 Ma in a pegmatite which was related to this unit.

3. Materials and methods

3.1. Samples

The tourmaline crystals were acquired from the mineralogical collection at the Institute of Geosciences of the University of Brasília. The samples are from central Brazil, in an area recently defined as the Mata Azul Pegmatitic Field by Queiroz (2016), where in the past, some pegmatites were intensely explored and produced gemstone varieties of tourmaline and beryl. However, there is no further information about the exact sampling location.

Five different types of tourmaline samples were studied:

- MA5: black tourmaline,
- MA5G: blue tourmalines,
- MA1G: dark green tourmalines,
- MA0: light green tourmalines,
- MA8: pink tourmalines.

Thin sections were made of one sample from each group. Each section was coated with a 25 nm-thick carbon film for electron microprobe analysis.

Several tourmaline crystals from each group were finely ground together using an agate mortar and pestle, with the exception of MA5 for which only one crystal was used. The powder material was then used for Mössbauer and UV-VIS spectroscopy analyses.

3.2. Electron-microprobe analyses

The chemical composition of tourmalines was analyzed with a JEOL JXA-8230 electron microprobe at the Electron Microprobe Laboratory in the Institute of Geosciences of the University of Brasília, with wavelength-dispersive spectrometer system operating at an accelerating potential of 15 kV and a beam current of 10^{-8} A. The samples were analyzed using the following standards: albite (Na), forsterite (Mg), topaz (F), anorthite (Al), microcline (Si, K), andradite (Ca, Fe), vanadinite (Cl, V), pyrophanite (Ti, Mn), Cr_2O_3 (Cr) and ZnO (Zn). The detection limits were up to 0.01 wt. % for Cl; 0.01 wt. % for Na, Mg, Al, Si, Ca, K, Fe and V; 0.02 wt. % for Zn; 0.01–0.02 wt. % for Mn and F, 0.01–0.03 wt. % for Cr and 0.02–0.05 wt. % for Ti. The mineral formulae were calculated based on 31 anions (O, OH, F), assuming $B = 3$ apfu (atoms per formula unit), $(\text{OH} + \text{F}) = 4$ apfu and $\text{Li} = 15 - (T + Z + Y)$ using the Excel™ worksheet of Tindle et al. (2002). Finally, all formulae were classified according to the rules of Henry et al. (2011).

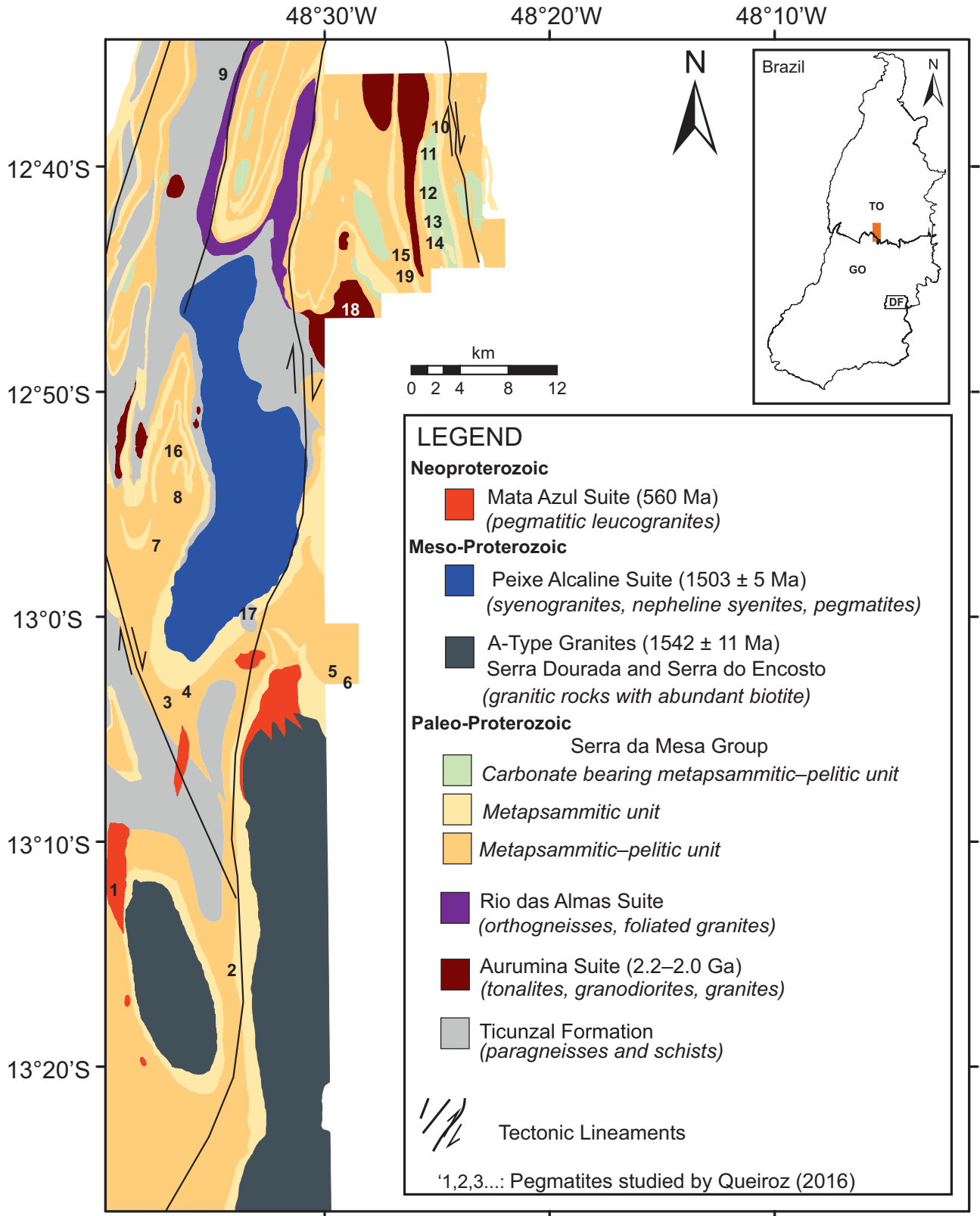
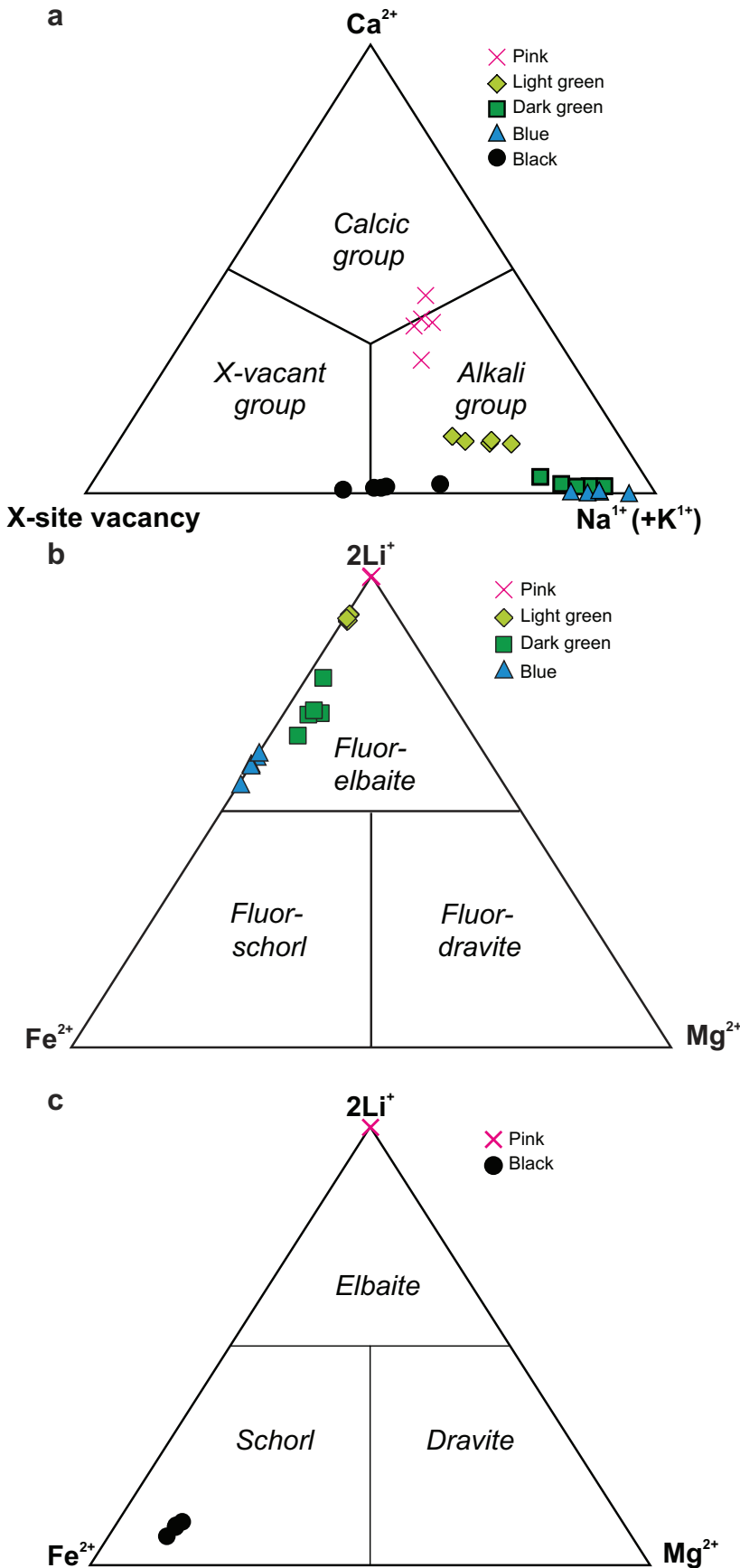


Fig. 1 Geological map of the Mata Azul Pegmatitic Field area with specific pegmatites studied by Queiroz (2016) represented with the numbers. 1: Levantina quarry, 2: Córrego das Pedras, 3: Jóia da Mata, 4: “four”, 5: “five”, 6: “six”, 7: São Júlio, 8: Pichorra, 9: Fazenda Mesquita, 10: Berilão, 11: Marta Rocha, 12: Zé do Fole, 13: Índio, 14: Boanerges, 15: Marimbondo, 16: “sixteen”, 17: “seventeen”, 18: Onça, 19: Marimbondinho (Queiroz and Botelho in print).



3.3. Mössbauer spectroscopy

Mössbauer spectra were acquired at room temperature (298 K) using a conventional spectrometer system with a ⁵⁷Co/Rh source providing an activity of 95 mCi at the Nuclear Technology Development Center (CDTN), Minas Gerais, Brazil. Analytical data were recorded in a multichannel analyzer using 1024 channels for the variable velocity range. The run-times were often 1–2 days; however, one week was used for the sample with the lowest Fe content. The isomer shifts and the velocity scale were calibrated against α-Fe foil at room temperature.

3.4. Optical spectroscopy in ultraviolet–visible range (UV-VIS)

The UV-VIS optical absorption spectra of the powder samples were obtained in the spectral range of 200–800 nm (50000–12500 cm⁻¹) using a UV 3600 Shimadzu spectrometer at the Department of Physics of the Federal University of Minas Gerais.

4. Results

4.1. Electron-microprobe analyses

The compositions of tourmaline samples are slightly heterogeneous in terms of both X- and Y-site occupancies (Fig. 2). All tourmalines belong to the alkali group with X-site dominated by Na, except two outlying points (Fig. 2a). The amount of X-site vacancy decreases from black, through green to blue tourmalines; the pink tourmaline has high contents of Ca as well as elevated amount of X-site vacancy (Fig. 2a). The W-site occupancy

Fig. 2 Classification diagrams for tourmaline; **a** – Diagram based on the occupancy of the X site, **b** – Ternary fluor-dravite–fluor-schorl–fluor-elbaite subsystem, and **c** – Ternary dravite–schorl–elbaite subsystem (Henry et al. 2011). The points corresponding to fluor-liddicoatite and foitite are not represented in the final graphics.

Tab. 1 Representative electron-microprobe analyses of black, blue, dark green, light green and pink tourmalines (wt. % and *apfu*)

	Black	Blue	Dark green	Light green	Pink
SiO ₂	35.03	36.23	37.05	38.34	36.70
TiO ₂	0.24	b.d.l.	0.36	0.30	0.06
Al ₂ O ₃	34.20	35.99	37.50	39.24	40.40
V ₂ O ₃	0.03	b.d.l.	0.04	b.d.l.	0.03
Cr ₂ O ₃	b.d.l.	0.07	0.05	b.d.l.	b.d.l.
FeO	14.06	8.73	4.76	1.91	0.05
MgO	1.11	0.04	0.71	0.03	0.01
CaO	0.12	0.01	0.12	0.70	2.17
MnO	0.24	0.40	0.57	0.93	0.59
ZnO	0.07	0.33	0.07	0.06	0.08
Na ₂ O	1.87	2.75	2.64	2.13	1.26
K ₂ O	0.03	0.03	0.01	0.02	0.02
F	0.27	1.38	1.20	1.26	1.10
Cl	b.d.l.	b.d.l.	b.d.l.	0.01	0.01
H ₂ O*	3.47	3.00	3.16	3.22	3.24
B ₂ O ₃ *	10.42	10.58	10.81	11.06	10.90
Li ₂ O*	0.18	1.16	1.53	2.08	2.26
Total	101.33	100.68	100.57	101.29	98.85
O=F	0.11	0.58	0.50	0.53	0.46
Total*	101.21	100.10	100.07	100.76	98.39
Structural formulae based on 31 anions (O, OH, F)					
T: Si	5.84	5.95	5.96	6.02	5.85
Al	0.16	0.05	0.04	–	0.15
B: B	3.00	3.00	3.00	3.00	3.00
Z: Al	6.00	6.00	6.00	6.00	6.00
Y: Al	0.57	0.92	1.06	1.26	1.45
Ti	0.03	b.d.l.	0.04	0.04	0.01
V	b.d.l.	b.d.l.	0.01	b.d.l.	b.d.l.
Cr	b.d.l.	0.01	0.01	b.d.l.	b.d.l.
Mg	0.28	0.01	0.17	0.01	b.d.l.
Mn	0.03	0.05	0.08	0.12	0.08
Fe _{total}	1.96	1.20	0.64	0.25	0.01
Zn	0.01	0.04	0.01	0.01	0.01
Li*	0.12	0.77	0.99	1.31	1.45
X: Ca	0.02	b.d.l.	0.02	0.12	0.37
Na	0.60	0.87	0.82	0.65	0.39
K	0.01	0.01	b.d.l.	b.d.l.	b.d.l.
□	0.37	0.12	0.16	0.23	0.24
I+/W: OH	3.86	3.28	3.39	3.37	3.45
F	0.14	0.72	0.61	0.63	0.55
Cl	b.d.l.	b.d.l.	b.d.l.	b.d.l.	b.d.l.
Species	Schorl	Fluor-elbaite	Fluor-elbaite	Fluor-elbaite	Fluor-elbaite

*Calculated by stoichiometry

All Fe was considered as FeO; b.d.l.= below detection limit; □ = vacancy

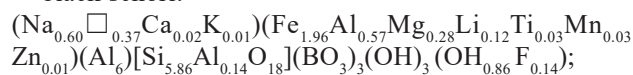
is dominated by F in all samples except the ^wOH-dominated black tourmaline with low F (0.06–0.27 wt. %) and one point of pink tourmaline. All samples show high Al contents (6.72–7.73 *apfu*). The representative analyses are shown in Tab. 1. The complete set of analyses is attached (Electronic Supplementary Material).

Following Henry et al. (2011), the black crystal varies between the schorl (Fig. 2c) and foitite species, the blue, dark green and light green tourmalines are classified as fluor-elbaite (Fig. 2b), and the pink tourmaline is transi-

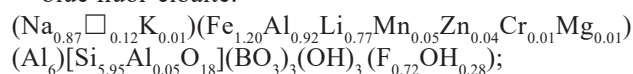
tional among fluor-elbaite (Fig. 2b), elbaite (Fig. 2c) and fluor-liddicoatite.

The representative structural formulae are as follows:

• black schorl:



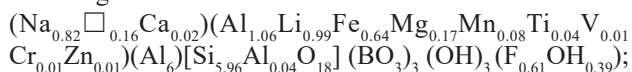
• blue fluor-elbaite:



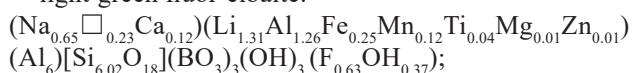
Tab. 2 Transition metal contents (wt. %) and Mn/(Mn + Fe) atomic ratios in the black, blue, dark green, light green and pink tourmalines

	FeO	MnO	TiO ₂	V ₂ O ₃	Cr ₂ O ₃	Mn/(Mn + Fe)
black	14.06	0.24	0.24	0.03	b.d.l.	0.02
	13.85	0.13	0.25	b.d.l.	0.07	0.01
	14.26	0.23	0.12	0.05	b.d.l.	0.02
	13.94	0.21	0.14	b.d.l.	0.08	0.01
	14.10	0.27	0.22	b.d.l.	b.d.l.	0.02
blue	8.27	0.42	0.15	b.d.l.	0.05	0.05
	7.94	0.44	b.d.l.	b.d.l.	b.d.l.	0.05
	8.73	0.40	b.d.l.	b.d.l.	0.07	0.04
	8.23	0.31	b.d.l.	b.d.l.	b.d.l.	0.04
	8.26	0.37	b.d.l.	0.01	b.d.l.	0.04
dark green	4.76	0.57	0.36	0.04	0.05	0.11
	3.78	1.00	0.26	b.d.l.	b.d.l.	0.21
	5.42	0.58	0.14	b.d.l.	0.02	0.10
	4.91	0.73	0.12	0.03	b.d.l.	0.13
	6.02	0.62	0.15	b.d.l.	b.d.l.	0.09
light green	1.67	1.18	0.11	0.04	0.06	0.42
	1.79	1.11	0.03	b.d.l.	0.05	0.38
	1.91	0.93	0.30	b.d.l.	b.d.l.	0.33
	1.84	0.88	0.09	0.05	b.d.l.	0.33
	1.88	0.97	0.07	0.04	0.05	0.34
pink	b.d.l.	0.27	b.d.l.	b.d.l.	b.d.l.	1.00
	0.05	0.59	0.06	0.03	b.d.l.	0.93
	b.d.l.	0.44	b.d.l.	0.02	0.05	1.00
	b.d.l.	0.48	b.d.l.	0.01	0.04	1.00
	0.05	0.11	0.03	b.d.l.	b.d.l.	0.68

• dark green fluor-elbaite:



• light green fluor-elbaite:



Tab. 3 Room-temperature ⁵⁷Fe Mössbauer parameters of the four analyzed tourmaline samples

Sample	δ (mm/s)*	Δ (mm/s)	T (mm/s)	A (%)	Iron valence
black	1.1	2.47	0.28	40.97	Fe ²⁺ Y1
	1.08	2.13	0.36	29.49	Fe ²⁺ Y2
	1.07	1.54	0.42	17.27	Fe ²⁺ Y3
	0.78	1.22	0.66	12.27	Fe ^{2.5+}
dark blue	1.06	2.38	0.37	65.36	Fe ²⁺ Y1
	1.15	2.29	0.33	27.26	Fe ²⁺ Y2
	1.06	1.28	0.57	7.38	Fe ^{2.5+} or Fe ²⁺ (?)
dark green	1.04	2.49	0.33	29.07	Fe ²⁺ Y1
	1.11	2.34	0.33	61.77	Fe ²⁺ Y2
	1.13	1.71	0.43	9.16	Fe ²⁺ Y3
light green	1.07	2.45	0.31	58.41	Fe ²⁺ Y1
	1.13	2.33	0.31	35.16	Fe ²⁺ Y2
	1.13	1.60	0.34	6.43	Fe ²⁺ Y3

Parameters of Mössbauer spectra:

δ – Isomer Shift, Δ – Quadrupole Splitting, τ – Peak Width, A – relative area

*Calibrated on α-Fe

• pink fluor-elbaite:

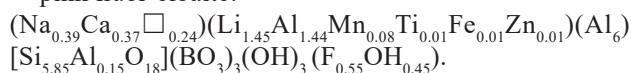


Table 2 summarizes ranges of contents of main chromophore transition metals found in the analyzed samples. The FeO content decreases in the following order: black (13.85–14.26 wt. %), blue (7.94–8.73 wt. %), dark green (3.78–6.02 wt. %), light green (1.67–1.91 wt. %), and pink (up to 0.05 wt. %).

The light green sample has the highest MnO content (0.88–1.18 wt. %), followed by dark green (0.57–1.00 wt. %), pink (0.11–0.59 wt. %), blue (0.31–0.44 wt. %) and black (0.13–0.27 wt. %). However, the only sample with greater MnO contents than those of FeO is the pink fluor-elbaite, which has the highest Mn/(Mn+Fe) atomic ratio (0.68–1.00), followed by the light green (0.33–0.42), dark green (0.9–0.21), blue (0.04–0.05) and black (0.01–0.02) samples.

The dark green sample has the highest TiO₂ content (0.12–0.36 wt. %), followed by the light green (up to 0.3 wt. %), black (0.12–0.25 wt. %), blue (up to 0.15 wt. %) and pink samples (up to 0.06 wt. %).

All the studied tourmalines show low contents of V₂O₃ (up to 0.05 wt. %) and Cr₂O₃ (up to 0.08 wt. %) or values below the detection limit of 0.01 wt. % for V₂O₃ and 0.01–0.03 wt. % for Cr₂O₃.

4.2. Mössbauer spectroscopy

The studied powder samples generated well-defined asymmetric doublet-shaped spectra (Fig. 3a–d), fitted with 3 or 4 doublets. The exception was the pink sample, from which it was not possible to acquire a spectrum, due to its very low iron content.

The hyperfine parameters for the analyzed tourmalines

are listed in Tab. 3. All fitted spectra provide three similar doublets, with the exception of the third doublet of blue tourmalines (isomer shift, δ = 1.06 mm/s and quadrupole splitting, Δ = 1.28 mm/s). The first common doublet has an δ varying between 1.04 and 1.1 mm/s, and a Δ between 2.38 and 2.49 mm/s, the second yielded δ of 1.08–1.15 mm/s and Δ of 2.13–2.34 mm/s and the third gave δ of 1.07–1.13 mm/s, and Δ of 1.54–1.71 mm/s. Additionally, the spectrum from the black sample features a fourth different doublet with δ = 0.78 mm/s and Δ = 1.22 mm/s.

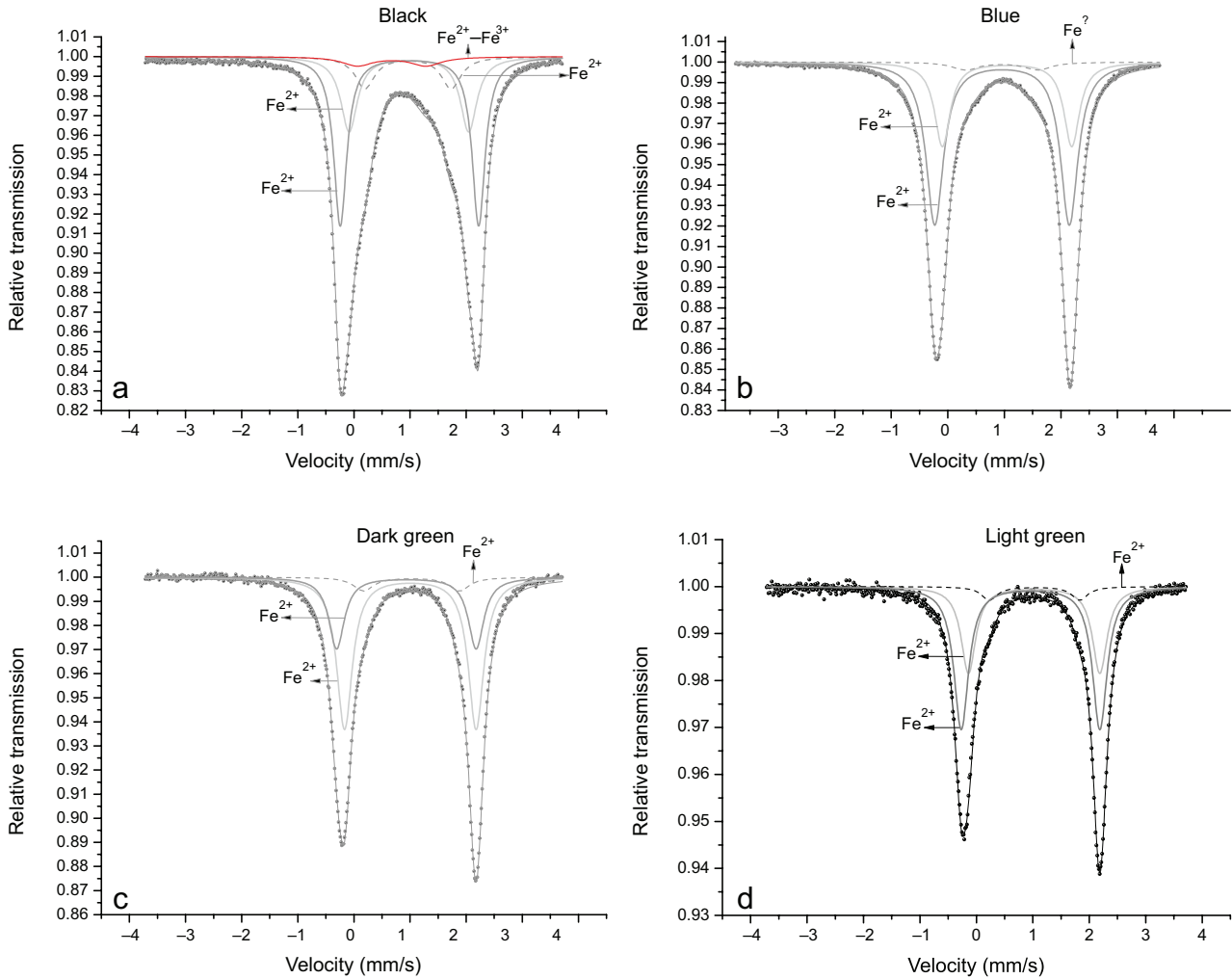


Fig. 3 Room-temperature Mössbauer spectra for black tourmaline (a), blue tourmalines (b) dark green tourmalines (c) and light green tourmalines (d).

4.3. Optical spectroscopy (UV-VIS)

The optical spectra of all the powdered tourmalines show intense UV absorption edges (Figs 4–5).

The spectrum of the black tourmaline shows a very high absorbance in the entire visible region. Prominent bands at *c.* 780 nm, 730 nm, 670 nm as well as smaller bands at *c.* 550 nm and 430 nm were observed (Fig. 4). The spectrum of blue tourmalines displays bands at *c.* 730 nm and 670 nm as well as very weak bands at 550 nm and

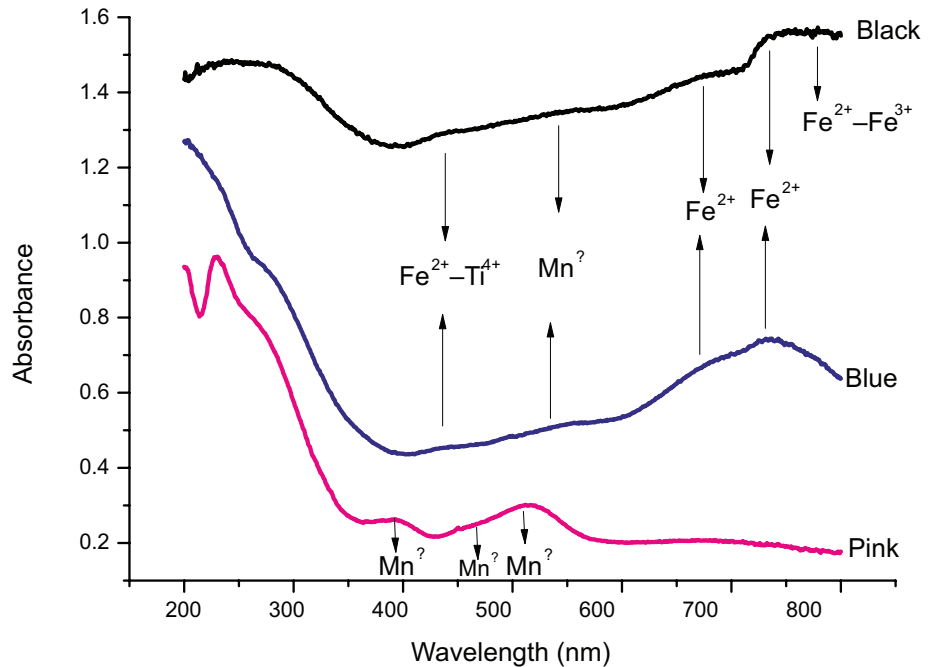


Fig. 4 Optical spectra from black, blue and pink tourmalines.

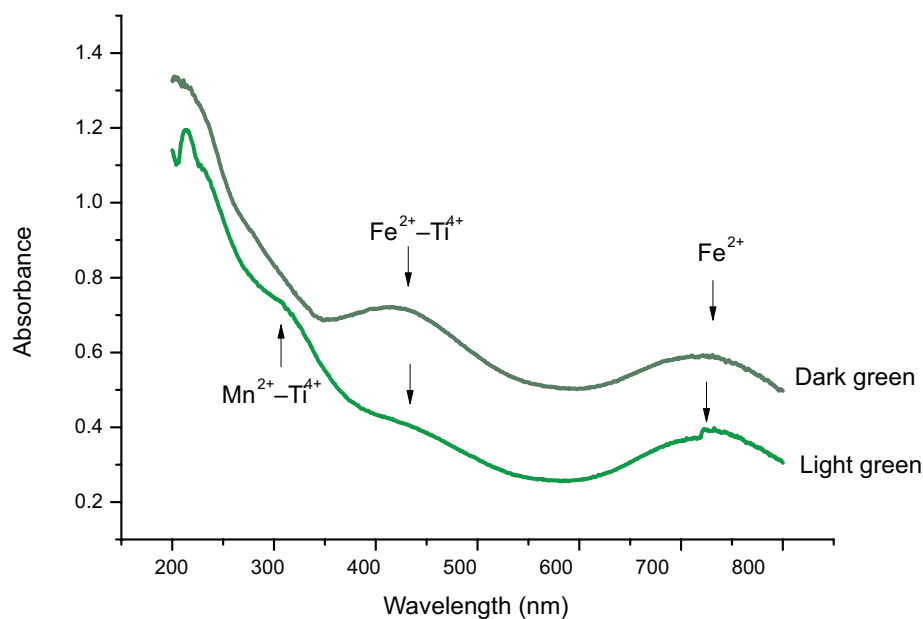


Fig. 5 Optical spectra from dark green and light green tourmalines.

430 nm (Fig. 4). The spectrum of pink tourmalines (Fig. 4) yielded absorption bands at *c.* 395 nm, 460 nm and 512 nm.

The spectra of light green and dark green tourmalines (Fig. 5) feature two main common absorption bands: at *c.* 430 nm and *c.* 730 nm that are more intense in the latter sample. Additionally, there is a band at 320 nm in the light green spectrum overlapping partly with its UV absorption edge.

5. Discussion

As the studied tourmaline crystals have very low contents of V_2O_3 and Cr_2O_3 (up to 0.08 wt. %), the main transition metals that could contribute to the color origin are Fe, Mn and Ti.

The decreasing FeO content can be related to the colors in the following order: black, blue, dark green and light green. Because the pink sample shows the highest Mn–Fe fractionation, and the lowest FeO and TiO_2 contents (with only amounts of the order 0.0X wt. %), the transitions related to the Fe and Ti are expected to have very low intensities, and the Mn is considered to be the main transition metal of this color.

Regarding the Mössbauer spectroscopy results (Tab. 3), the three doublets from dark green and light green tourmaline spectra were ascribed to Fe^{2+} at *Y* site with different nearest-neighbor coordination environments (following Dyar et al. 1998; Pieczka et al. 1998; Castañeda et al. 2006b; Andreozzi et al. 2008). This interpretation agrees with various structure refinement studies performed on Li-bearing tourmalines which showed that the *Z* site is typically fully populated by Al (e.g., Bosi et al. 2013; Ertl et al. 2013).

The Mössbauer spectra are mutually well comparable except for two doublets in black ($\delta = 0.78$ mm/s and $\Delta = 1.22$ mm/s) and blue ($\delta = 1.06$ mm/s and $\Delta = 1.28$ mm/s) tourmalines with rather low values of quadrupole splitting Δ (Tab. 3). Doublets similar to the former have been commonly related to electron delocalization and they have been mainly ascribed to $Fe^{2.5+}$, i.e. intervalence charge transfer (IVCT) interactions, at least partly, between Fe^{2+} and Fe^{3+} ions located in adjacent sites (e.g., Saegusa et al. 1979; Kraczka and Pieczka 2001; Andreozzi et al. 2008; Filip et al. 2012). Therefore, we relate the fourth doublet of the black tourmaline spectrum to Fe^{2+} – Fe^{3+} IVCT.

On the other hand, the third doublet in the blue tourmaline spectrum could represent either $Fe^{2.5+}$ or Fe^{2+} at the *Z* site; neither of these assignments matches well with the ranges listed in the comprehensive study of Andreozzi et al. (2008). However, it most likely represents $Fe^{2.5+}$ at the *Y* adjacent sites, with regard to the study of Watenphul et al. (2017) who showed that especially in the elbaite structure, Fe^{2+} has a very small tendency for disorder over the *Y* and *Z* sites. Some studies (e.g. Pieczka et al. 1998) also assigned doublets with low quadrupole splitting values (down to about 1.2 mm/s) to the presence of Fe^{2+} at *Y* site. In any case, the doublet δ and Δ values are anomalous and cannot be unequivocally interpreted based solely on the Mössbauer data.

Based on the literature data (Taran et al. 2015), the intense UV absorption edge shown in all our optical spectra could originate from some electronic charge-transfer transitions of the ligand-to-metal type. However, it is not possible to decipher which cation is involved in this process as all samples show the same feature.

The absorbance of the spectra in the 730 nm region correlates positively with the FeO contents determined

Tab. 4 Interpretation of the optical spectroscopy results combined with Mössbauer spectroscopy and the main transition metal contents

Color	FeO (wt. %)	TiO ₂ (wt. %)	MnO (wt. %)	Mössbauer	Main absorption bands	Likely assignments
black	13.85–14.26	0.12–0.25	0.13–0.27	Fe ²⁺ (Y1), Fe ²⁺ (Y2), Fe ²⁺ (Y3)	~730 nm, ~670 nm	Fe ²⁺ d–d transition
					~780 nm	Fe ²⁺ –Fe ³⁺ IVTC
					~550 nm	Mn ²⁺ d–d transition
					~430 nm	Fe ²⁺ –Ti ⁴⁺ IVTC
blue	7.94–8.73	0.00–0.15	0.31–0.44	Fe ²⁺ (Y1), Fe ²⁺ (Y2), Fe ^{2.5+} or Fe ²⁺ (?)	~730 nm, ~670 nm	Fe ²⁺ d–d transition
					~550 nm	Mn ²⁺ d–d transition
					~430 nm	Fe ²⁺ –Ti ⁴⁺ IVTC
dark green	3.78–6.02	0.12–0.36	0.57–1.00	Fe ²⁺ (Y1), Fe ²⁺ (Y2), Fe ²⁺ (Y3)	~730 nm	Fe ²⁺ d–d transition
					~430 nm	Fe ²⁺ –Ti ⁴⁺ IVTC
light green	1.67–1.91	0.03–0.30	0.88–1.18	Fe ²⁺ (Y1), Fe ²⁺ (Y2), Fe ²⁺ (Y3)	~730 nm	Fe ²⁺ d–d transition
					~430 nm	Fe ²⁺ –Ti ⁴⁺ IVTC
					~320 nm	Mn ²⁺ –Ti ⁴⁺ IVTC
pink	0.00–0.05	0.00–0.06	0.11–0.59	–	~395 nm	Mn ²⁺ d–d transition
					~460 nm	or
					~512 nm	Mn ²⁺ –Mn ³⁺ IVTC

by the EMPA as they increased in the same order: light green, dark green, blue and black. Bands in this region are often related to Fe²⁺ (e.g., Mattson and Rossman 1987; Castañeda et al. 2006b). Therefore, in accordance with the our results of Mössbauer spectroscopy that indicate the presence of ferrous iron in all these samples, the bands at *c.* 730 nm and 670 nm (Tab. 4) are assigned to d–d electronic transitions of Fe²⁺.

A Fe²⁺–Fe³⁺ IVCT is considered to be the cause of the absorption at 780 nm in the optical spectra of the black tourmaline based on the Mössbauer spectroscopy results.

The band at 430 nm that is prominent in the optical spectra of the dark green and light green tourmalines, is assigned to Fe²⁺–Ti⁴⁺ IVCT following Rossman and Mattson (1986), Mattson and Rossman (1988) and Rossman (2014). This assignment is corroborated by the chemical data, since the FeO and TiO₂ contents are greater in the dark green sample than in the light green one, similarly to the intensity of this band (Fig. 5, Tab. 4). In addition, band near 320 nm is assigned to the Mn²⁺–Ti⁴⁺ charge transfer (Rossman and Mattson 1986), considering that the light green tourmaline has the greatest MnO content among all the tourmaline varieties studied here (Tab. 4).

Absorption bands at *c.* 395 nm and 512 nm were already assigned in previous pink tourmaline studies to d–d transitions of Mn³⁺ at the Y sites (e.g., Liu et al. 2011; Maneewong et al. 2016), and bands at *c.* 460 and 520 nm were related to transitions of Mn²⁺ in magnetically non-equivalent sites (Castañeda et al. 2006a). The pink color in tourmalines could also result from intervalence charge transfer between Mn²⁺ and Mn³⁺ (see review of Pezzotta and Laurs 2011). Thus, it is still possible that some of the bands encountered in the pink spectra could span from Mn²⁺–Mn³⁺ IVCT.

A band at 550 nm, found in blue and black tourmaline spectra, is also related to the transitions of Mn cations.

6. Conclusions

Tourmalines from the Mata Azul Pegmatitic Field, central Brazil, with different colors were characterized using electron-microprobe analyses, Mössbauer spectroscopy and ultraviolet–visible range (UV-VIS) optical spectroscopy. The following conclusions were obtained:

- The black color is formed by high absorbance in all regions of the visible spectra caused by Fe²⁺–Fe³⁺ IVCT (780 nm), Fe²⁺d–d transitions (730 nm, 670 nm), Fe²⁺–Ti⁴⁺ IVCT (430 nm) and transitions related to Mn cations (550 nm);
- The blue color is distinguished from green colors by the higher absorbance in the 730 nm region (Fe²⁺d–d transitions), and the higher FeO content, as well as a lower absorbance in the 430 nm region and a lower TiO₂ content;
- The green colors are associated with absorption bands at 730 nm (Fe²⁺ d–d transitions) and 430 nm (Fe²⁺–Ti⁴⁺ IVCT);
- The light green color has a lower absorbance compared to the dark green and an additional band at 320 nm (Mn²⁺–Ti⁴⁺ IVCT);
- The pink color is a result of the high Mn–Fe fractionation. It was not possible to assure the oxidation states of the Mn cations. The existence of Mn²⁺–Mn³⁺ IVCT is also possible.

This work contributes to increasing the available comprehensive chemical and spectroscopic data of tourmalines. Furthermore, this is the first detailed chemical and spectroscopy study of tourmalines from the granitic

pegmatites of central Brazil. The results can be used to support future studies in treatments for color enhancement in tourmalines from the Mata Azul Pegmatitic Field and in similar tourmalines.

Acknowledgements. The FAP-DF Ms.C scholarship to Simone F. da Silva is gratefully acknowledged. We are indebted to Nilson F. Botelho for the electron-microprobe analysis and the beneficial discussion, to Cristiano Fantini for allowing us to use the UV-VIS laboratory and to Professor Geraldo Rezende de Andrade *in memoriam*, to whom the tourmaline samples belonged before they were stored at the Institute of Geosciences of the University of Brasília. We also want to thank Andy Tindle, Julie Selway and Jian Xiong for the Excel™ worksheet used for the calculation of structural formulae of tourmaline (downloaded from Tindle's website), the handling editor J. Cempírek for improving the quality of the manuscript and the reviewers J. Fridrichová and A. Pieczka for their advices and fruitful suggestions.

Electronic supplementary material. A table containing the complete electron-microprobe analyses of the studied tourmalines is available online at the Journal web site (<http://dx.doi.org/10.3190/jgeosci.258>).

References

- ALVARENGA CJS, BOTELHO NF, DARDENE MA, LIMA ONB, MACHADO MA (2007) Geologia da folha Cavalcante SD.23-V-C-V 1: 100.000
- ANDREOZZI GB, BOSI F, LONGO M (2008) Linking Mössbauer and structural parameters in elbaite-schorl-dravite tourmalines. *Amer Miner* 93: 658–666
- BOSI F, ANDREOZZI GB, SKOGBY H, LUSSIER AJ, ABDU Y, HAWTHORNE FC (2013) Fluor-elbaite, $\text{Na}(\text{Li}_{1.5}\text{Al}_{1.5})\text{Al}_6(\text{Si}_6\text{O}_{18})(\text{BO}_3)_3(\text{OH})_3\text{F}$, a new mineral species of the tourmaline supergroup. *Amer Miner* 98: 297–303
- CASTAÑEDA C (2002) Caracterização Mineralógica de Amostras Naturais e Tratadas de Turmalinas e Morganitas do Distrito Pegmatítico de Araçuaí, Minas Gerais. Unpublished PhD Thesis, Universidade de Brasília, Brasília, pp 1–230
- CASTAÑEDA C, BOTELHO NF, KRAMBROCK K, DANTAS MS, PEDROSA-SOARES AC (2006a) Centros paramagnéticos em elbaíta rosa natural e irradiada. *GEONOMOS* 14: 7–15
- CASTAÑEDA C, ECKHOUT SG, DA COSTA GM, BOTELHO, NF, DE GRAVE, E (2006b) Effect of heat treatment on tourmaline from Brazil. *Phys Chem Miner* 33: 207–216
- CUADROS FA, BOTELHO NF, FUCK RA, DANTAS EL (2017a) The Ticunzal Fm. in central Brazil: record of Rhyacian sedimentation and metamorphism in the western border of the São Francisco Craton. *J South Am Earth Sci* 79: 307–325
- CUADROS FA, BOTELHO NF, FUCK RA, DANTAS EL (2017b) The peraluminous Aurumina Granite Suite in central Brazil: an example of mantle–continental crust interaction in a Paleoproterozoic Cordilleran hinterland setting? *Precambr Res* 299: 75–100
- ČERNÝ P (1990) Distribution, affiliation and derivation of rare-element granitic pegmatites in the Canadian Shield. *Geol Rundsch* 79: 183–226
- ČERNÝ P (1991) Rare-element granitic pegmatites. Part I Anatomy and internal evolution of pegmatite deposits. *Geosci Can* 18: 49–67
- ČERNÝ P, ERCIT TS (2005) The classification of granitic pegmatites revisited. *Canad Mineral* 43: 2005–2026
- DE ALMEIDA FFM, HASUI Y, DE BRITO NEVES BB, FUCK RA (1981) Brazilian structural provinces: an introduction. *Earth Sci Rev* 17: 1–29
- DARDENE MA (2000) The Brasília Fold Belt. In: COR-DANI UG, MILANI EJ, THOMAZ FILHO A, CAMPOS DA (eds) Tectonic Evolution of South America. 31st International Geological Congress, SBG, Rio de Janeiro, pp 231–263
- DYAR MD, TAYLOR ME, LUTZ TM, FRANCIS CA, GUIDOTTI CV, WISE M (1998) Inclusive chemical characterisation of tourmaline: Mössbauer study of Fe valence and site occupancy. *Amer Miner* 83: 848–864
- ERTL A, GIESTER G, SCHÜSSLER U, BRÄTZ H, OKRUSCH M, TILLMANN E, BANK H (2013) Cu- and Mn-bearing tourmalines from Brazil and Mozambique: crystal structures, chemistry and correlations. *Mineral Petrol* 107: 265–279
- FILIP J, BOSI F, NOVÁK M, SKOGBY H, TUČEK J, ČUDA J, WILDNER M (2012) Iron redox reactions in the tourmaline structure: high-temperature treatment of Fe^{3+} -rich schorl. *Geochim Cosmochim Acta* 86: 239–256
- HENRY DJ, DUTROW BL (2012) Tourmaline at diagenetic to low-grade metamorphic conditions: its petrologic applicability. *Lithos* 154: 16–32
- HENRY DJ, NOVÁK M, HAWTHORNE FC, ERTL A, DUTROW BL, UHER P, PEZZOTTA F (2011) Nomenclature of the tourmaline-supergroup minerals. *Amer Miner* 96: 895–913
- KRACZKA J, PIECZKA A (2001) Crystallochemical structure of tourmalines inferred from Mössbauer spectroscopy. *Acta Phys Pol A* 100: 743–750
- KRAMBROCK K, PINHEIRO MVB, MEDEIROS SM, GUEDES KJ, SCHWEIZER S, SPAETH JM (2002) Investigation of radiation-induced yellow color in tourmaline by magnetic resonance. *Nucl Instrum Methods Phys Res* 191: 241–245
- KRAMBROCK K, PINHEIRO MVB, MEDEIROS SM, GUEDES KJ, SCHWEIZER S, SPAETH JM (2004) Correlation of irradiation-induced yellow color with the O-hole center in tourmaline. *Phys Chem Miner* 31: 168–175

- LACERDA FILHO JV, RESENDE A, SILVA A (1999) Geologia e recursos minerais do estado de Goiás e Distrito Federal. Programa levantamentos geológicos básicos do Brasil. CPRM/METAGO/UnB, Goiânia, Mapa geológico e de recursos mineral, escala 1 : 500 000
- LIU X, FENG X, FAN J, GUO S (2011) Optical absorption spectra of tourmaline crystals from Altay, China. *Chinese Opt Lett* 9: 1–4
- MANEAWONG A, SEONG BS, SHIN EJ, KIM JS, KAJORNRIITH V (2016) Color change of tourmaline by heat treatment and electron beam irradiation: UV–Visible, EPR, and Mid-IR spectroscopic analyses. *J Korean Phys Soc* 68: 83–92
- MARQUES G (2009) Geologia dos Grupos Arai e Serra da Mesa e Seu Embasamento no Sul de Tocantins. Unpublished MSci thesis, University of Brasília, Brasília, pp 1–116
- MATTSON SM, ROSSMAN GR (1987) Fe²⁺–Fe³⁺ interactions in tourmaline. *Phys Chem Miner* 14: 163–171
- MATTSON SM, ROSSMAN GR (1988) Fe²⁺–Ti⁴⁺ charge transfer in stoichiometric Fe²⁺, Ti⁴⁺-minerals. *Phys Chem Miner* 16: 78–82
- PEZZOTTA F, LAURS BM (2011) Tourmaline: the kaleidoscopic gemstone. *Elements* 7: 333–338
- PIECZKA A, KRACZKA J, ŻABIŃSKI W (1998) Mössbauer spectra of Fe³⁺-poor schorls: reinterpretation on the basis of ordered structure model. *J Czech Geol Soc* 43: 69–74
- POLO HJO, DIENER FS (2013) Carta geológica: folha Mata Azul SD.22-X-DII. Projeto Noroeste de Goiás, CPRM-Companhia de Pesquisa de Recursos Minerais, Goiânia
- QUEIROZ HA (2016) Sistema Granítico–Pegmatítico Mata Azul: Caracterização e Gênese. Unpublished PhD thesis, University of Brasília, Brasília, pp 1–131
- QUEIROZ HA, BOTELHO NF (2017) Fosfatos de Fe e Mn primários e secundários em pegmatitos graníticos do Campo Pegmatítico Mata Azul, Jaú do Tocantins, TO, Brasil. *Geol USP Série Científica* 17: 159–168
- QUEIROZ HA, BOTELHO NF (in print) The Mata Azul pegmatitic field, Tocantins/Goiás, central Brazil: geology, genesis and mineralization. *Brazil J Geol* (doi: 10.1590/2317-4889201820170048)
- ROSSMAN GR (2014) Optical spectroscopy. In: HENDERSON GS, NEUVILLE DR, DOWNS RT (eds) *Spectroscopy Methods in Mineralogy and Materials Sciences. Reviews in Mineralogy and Geochemistry* 78: 371–398
- ROSSMAN GR, MATTSON SM (1986) Yellow, Mn-rich elbaite with Mn–Ti intervalence charge transfer. *Amer Miner* 71: 599–602
- SAEGUSA N, PRICE D, SMITH G (1979) Analysis of the Mössbauer spectra of several iron-rich tourmalines (schorls). *J Phys Colloques* 40: C2-456–C2-459
- TARAN MN, DYAR MD, NAUMENKO I V., VYSHNEVSKY OA (2015) Spectroscopy of red dravite from northern Tanzania. *Phys Chem Miner* 42: 559–568
- TINDLE AG, BREAKS FW, SELWAY JB (2002) Tourmaline in petalite-subtype granitic pegmatites: evidence of fractionation and contamination from the Pakeagama Lake and Separation Lake areas of northwestern Ontario, Canada. *Canad Mineral* 40: 753–788
- VALERIANO CM, DARDENNE MA, FONSECA MA, SIMÕES LSA, SEER HJ (2004) A evolução tectônica da Faixa Brasília. In: MANTESSO-NETO V, BARTORELLI A, CARNEIRO CDR, BRITO-NEVES BB (eds) *Geologia do Continente Sul-Americano: Evolução da Obra de Fernando Flávio Marques de Almeida*. Beca, São Paulo, pp 575–593
- WATENPHUL A, MALCHEREK T, WILKE FDH, SCHLÜTER J, MIHAILOVA B (2017) Composition–thermal expandability relations and oxidation processes in tourmaline studied by in situ Raman spectroscopy. *Phys Chem Miner* 44: 735–748